Protoplasma (2020) 257:157–167
https://doi.org/10.1007/s00709-019-01423-w

ORIGINAL ARTICLE

Elevated expression of cellular SYNE1, MMP10, and GTPase1 and their regulatory role in hepatocellular carcinoma progression

Laila H. Faraj Shaglouf[1] · Maryam Ranjpour[1] · Saima Wajid[1] · Swatantra Kumar Jain[2]

Received: 12 April 2019 / Accepted: 19 July 2019 / Published online: 19 August 2019

Abstract

Hepatocellular carcinoma (HCC) is the most common primary liver malignancy resulting in high mortality. HCC progression is associated with abnormal signal transduction that changes cell signaling pathways and ultimately leads to dysregulation of cell functions and uncontrolled cell proliferation. Present study was undertaken with the objective to identify differentially expressed proteins and quantify their transcript expression in the liver of HCC-bearing rats vis-à-vis controls and to decipher the network involving interaction of genes coding for the characterized proteins to an insight into mechanism of HCC tumorigenesis. 2D-Electrophoresis and MALDI-TOF-MS/MS were used to characterize differentially expressed proteins in DEN (diethylnitrosamine)-induced HCC tissue using the protocol reported by us earlier. Real-time PCR was performed to quantify the expression of transcripts for the identified proteins. GENEMANIA, an interacting network of genes coding for selected proteins, was deciphered that provided the functional role of these proteins in HCC progression. Upregulation of proteins SYNE1, MMP10, and MTG1 was observed. The mRNA quantification revealed elevated expression of their transcripts at HCC initiation, progression, and tumor stages. Network analysis showed the involvement of the genes coding for these proteins in dysregulation of signaling pathways during HCC development. The elevated expression of SYNE1, MMP10, and MTG1 suggests the role of these proteins as potential players in HCC progression and tumorigenesis.

Keywords Hepatocellular carcinoma · SYNE1 · MMP10 · MTG1 and gene interaction network

Introduction

Hepatocellular carcinoma (HCC) is the cause of high number of cancer-related deaths worldwide. As per the latest annual GLOBOCON statistics, the mortality rate of hepatocellular carcinoma among all cancer types is 8.2% (781,631 deaths in 2018); this figure very close to new HCC incidence of 841,080 cases in 2018 (Bray et al. 2018). The lack of markers for its early diagnosis results in usually only at advanced stage detection of HCC that makes the patient's survival limited and higher mortality rate seems inevitable (Hemming et al. 2016). During the last 10 years, the emergence of HCC has been in proportion to the prevalence and perpetuation of exposure to hepatitis B and C (Hemming et al. 2016). However, now, obesity and NAFLD either viral- or alcoholic-induced hepatitis are slowly becoming the primary causes of HCC (Younes and Bugianesi, 2018). The mass awareness about hepatitis A and hepatitis B vaccines and availability of high effective of direct antiviral therapies for HCV may have substantial impact in reducing the appearance of HCC in future (Hemming et al. 2016). It is well reported that most of the chronic diseases related to liver cancer are caused by changes at the phenotypic and genotypic levels in tumor cells. Further exploration of pathogenesis leading to HCC suggested that certain signaling pathways and molecular alterations have regulatory impact in HCC development by promoting cell growth and survival (Avila et al. 2006). Alterations in cell signaling pathways play a major role in tumorigenesis (Sever and Brugge, 2015), but mechanisms affecting cell signaling leading to

Handling Editor: Jörn Bullerdiek

Electronic supplementary material The online version of this article (https://doi.org/10.1007/s00709-019-01423-w) contains supplementary material, which is available to authorized users.

✉ Swatantra Kumar Jain
skjain@jamiahamdard.ac.in

[1] Department of Biotechnology, School of Chemical and Life Science, Jamia Hamdard, New Delhi 110062, India

[2] Department of Biochemistry, Hamdard Institute of Medical Science and Research, Jamia Hamdard, New Delhi 110062, India

hepatocarcinogenesis are still not fully understood (Samuele et al. 2013). The main lineaments of HCC are inflammation, ROS (reactive oxygen species), fibrosis, and cirrhosis that induce genetic and epigenetic mutations leading to activation of oncogenes and inhibition of tumor suppressor genes (Samuele et al.2013). P53/RB, Wnt/β-catenin, PI3K/PTEN/Akt/mTOR, JAK/STAT, MAPKs, RAS, ERK1/2, NF-κB, c-Myc, IGF1 and AP-1, retinoblastoma protein (pRb) chromatin regulation, oxidative and endoplasmic reticulum stress signaling, TGF-β, and HGF/c-Met are the main altered signaling pathways involved in HCC development (Aravalli et al. 2013; De Minicis. et al. 2013: Chiba et al. et al. 2015; Bakiri et al. 2017).

To identify the key players in pathogenesis of HCC, our laboratory has been trying to understand the signal transduction processes that lead to HCC initiation and progression, and to identify the tissue specific proteins that may have potential to serve as biomarker for early diagnosis and therapeutic targets of HCC. The present study was carried out using liver tissues from HCC-bearing male Wistar rats (Ranjpour et al. 2018). We earlier reported the development of a novel rodent model for study of HCC (Malik et al. 2013). Total tissue proteins were resolved on 2D gels, the differentially expressed proteins were analyzed by PD Quest, and protein spots of interest were characterized. The mRNA expression for the characterized proteins was quantified to validate the protein data obtained by 2D-Electrophoresis. Further, a global gene network has been developed to reveal the interactions among genes coding for the experimentally identified proteins and their interactors associated with signaling pathways during HCC progression.

Methods

The animal model for study of HCC was previously developed in our laboratory (Malik et al. 2013). The liver tissues were taken from HCC-bearing animals (Ranjpour et al. 2018). The study included 36 animals (Wistar rats) divided into two groups: control group and treated group, each group having 18 animals. The animals in treated group were further subdivided into three groups: 1 month, 2 month, and 4 month (6 animals in each group). The carcinogens DEN and 2-AFF (acetyl amino fluorine) were used to induce HCC. A single dose (200 mg/kg body weight) of DEN was given intravenously to each animal of treated group to initiate HCC, followed by oral doses of 2-AAF (150 mg/kg body weight) on the alternate days of first week of each month to promote HCC development. The control groups were treated with normal saline at the same schedule as the treated groups. The animals were sacrificed at the end of each month; liver tissues were excised and preserved in RNA *later solution* for further study (Ranjpour et al. 2019).

Proteomic profiling of proteins

We commenced our investigation based on *omics* approaches, wherein the liver tissues were preserved in RNA *later* s*olution* (RNA stabilization reagent from QIAGEN) and kept at − 80 °C until used. (100–150 mg) Tissues were homogenized using Polytron PT3100 homogenizer in the presence of urea lysis buffer (8 M urea, 65 mM CHAPS, 65 mM DTT, 2 M thiourea, 33 Mm Tris, and 6 mM PMSF). The homogenate was centrifuged (10,000 rpm for 10 min) (Chaudhary et al. 2013). The proteins extracted from the supernatant fraction were estimated by Bradford method (Bradford 1976). Aliquots containing 120 μg proteins were focused on 11-cm, pH 4–7 IPG strips (GE Healthcare, Immobilize TM Dry Strip) at 500 V for 1 h, at 1000 V for 1 h, and finally at 6000 V for a total of 35,000 V-hour. The total proteins were then fractionated using 12% gradient SDS polyacrylamide gels electrophoresis for 2D analysis of proteins. The resolved proteins were silver stained, analyzed by PD-Quest software (Bio-Rad), and the proteins of interest were characterized by MALDI-TOF-MS analysis as described earlier (Ranjpour et al. 2018).

Characterization of proteins by MALDI-TOF-MS/MS analysis

The protein spots identified by PD Quest analysis were excised and transferred to sterilized eppendorf tubes, destained by soaking the gel pieces in 15 mM potassium ferricyanide and 50 mM sodium thiosulphate, three times 10 min each. ACN (Acetonitrile) and a Speed Vac were used to thoroughly dehydrate and dry the gel pieces. These were further incubated for 1 h in DTT for rehydration followed by incubation in iodoacetamide for 45 min. The gel pieces were incubated for 10 min with ammonium bicarbonate, completely dehydrated with ACN, and dried. The proteins in gel pieces were digested with 150–200 ng trypsin in 50 mM ammonium bicarbonate for 16 h at 37 °C. The peptides were extracted with the peptide extraction solution and re-suspended in 20 mM of Tris-acetate buffer pH 7.5. The HCCA matrix was mixed with peptides that produced in 1:1 ratio and 2 μl of the mixture solution was applied on MALDI plate. Finally, samples were dried and analyzed by MALDI TOF/TOF Ultraflex III instrument version 3.2. The peptide mass fingerprint was fed into the Mascot server for a peptide mass fingerprint search in the NCBInr *Rattus norvegicus* database for protein characterization (Ranjpour et al. 2018).

Validation of expression of experimental protein findings using real-time PCR

Total RNA was isolated from 50 mg of liver tissue from control and treated group using Mini Sure Spin total RNA isolation kit (Nucleopore, Genetix Biotech Asia), RNA

concentration was measured using NanoDrop 2000c Spectrophotometer 56 (Thermo Fisher Scientific), and the purity of RNA was assessed by A260/A280 ratio. A sample containing 1500 ng RNA was reverse transcribed using cDNA synthesis kit (Verso cDNA Synthesis Kit, Thermo Scientific). The integrity of cDNA was confirmed by PCR amplification using GAPDH specific primers. Further, the primers were designed against the specific genes coding for the MALDI-TOF characterized proteins (Table 1). The PCR reaction mixture contained 0.5 μl cDNA, 1× Taq buffer, 1 U Taq polymerase, 1.5 mM MgCl2, 0.4 mM dNTPs, and 0.4 μM each primers; the amplification conditions were (i) 96 °C for 5 min (initial denaturation); (ii) 35 cycles of 94 °C for 30 s, 58 °C for 30 s, 72 °C for 30 s; and (iii) final extension 72 °C for 10 min. Amplified products were analyzed on 1.5% agarose gels by electrophoresis in 1× TAE buffer system and the DNA bands were visualized using UV gel documentation system (Alpha Imager HP System). Furthermore, the quantification of transcripts was carried out using Roche LightCycler 480 Real-Time PCR System using SYBR green chemistry. The data was analyzed using LightCycler 480 Software (Version 1.5). The 25 μl reaction mixture contained 12.5 μl of 2× Maxima SYBR Green qPCR Master Mix (Thermo Fisher Scientific), 0.4 μM of each primer (Table 1), 200 ng cDNA and nuclease free water. The thermal cycling conditions were (i) 95 °C for 10 min (initial denaturation), (ii) 45 cycles of 95 °C for 30 s, 56 °C for 30 s, and 72 °C for 30 s, followed by (iii) melt curve analysis at temperature range of 55–95 °C.

Mapped networks for SYNE1, MMP10, MTG1, and their interacting partners

Our major goal was to understand the functional involvement of the three selected proteins and their interacting partners with etiopathophysiology of HCC. We took the advantage of software GENEMANIA database to map our network (Warde-Farley et al. 2010). All the genes coding for selected proteins and their associated partners were mapped.

Table 1 The primers sequence of corresponding genes of MALDI-TOF identified proteins along with housekeeping gene primers

Gene name	Primer sequence	Amplicon size
GAPDH	F.P:ACTCTACCCACGGCAAGTTC R.P:GTGGTGAAGACGCCAGTAGA	163 bp
SYNE1	F.P:CCAGGCCAAAGTCCTAACCG R.P:CAGGTCATAGAGGCGGATGC	190 bp
MMP10	F.P:GATCTTGCTCAGCAATACCTAG R.P:TCACAATCCTGTAGGAGATGTG	265 bp
MTG1	F.P: TCCGTCTGCGAGCTCTTCCGA R.P: CTTTAGTCCCTTGGCCATGTGG	148 bp

The statistical analysis

In the real-time analysis, all the cDNA samples were run in triplicates. One-way ANOVA and post hoc Dunnet test were carried out by using GraphPad Prism (version 8); at $P < 0.05$, the difference between treated and control group was considered to be significant.

Results

Identification of the differentially expressed proteins

We earlier reported histological confirmation of HCC initiation at 1 month and tumorigenesis at 4 months after carcinogen treatment (Ranjpour et al. 2018). Total liver proteins of control and tumor-bearing rats were resolved on 2D gels (Fig. 1, A and B). Protein profiles were compared and analyzed using PD-Quest software. Differentially expressed proteins were identified, based on the difference in intensity of the spots. Three protein spots, namely, A, C, and E whose expression was elevated in tumor tissue, were selected for further studies. These spots were assigned unique SSP numbers by PD-Quest analysis (Fig. 1 C). The protein spots of interest were characterized to be nesprin-1 isoform X6 (Nesprin-1), stromelysin-2 precursor (Stromelysin-2), and mitochondrial ribosome–associated GTPase 1-isoform X2 respectively (Fig. 2). These proteins and their genes are listed in Table 2. The peptide sequence analysis of these proteins has been represented in Table 3.

Transcript quantification of differentially expressed proteins

The qPCR analysis revealed elevated expression of the transcripts for all the target proteins in tumor tissues. A 2.9-fold increase in expression of transcript for MMP10 was seen at 1-month post-carcinogen treatment. The mRNA expression continued to increase with disease progression and showed 3.7-fold elevation at 2-month and 5.4-fold increase at 4-month post-carcinogen treatment. Similarly, quantification of mRNA for MTG1 revealed 2.3-fold increase at 1-month, 4.7-fold increase at 2-month, and 5.1-fold increase at 4-month post-carcinogen treatment. On the other hand, the analysis of mRNA expression for SYNE1 revealed 1.33-fold increase at 1 month after carcinogen treatment. However, its transcript expression then plateaued and remained elevated almost at the same level during HCC progression and tumorigenesis. The analysis revealed 1.28-fold increase at 2-month and 1.74-fold increase at 4-month post-carcinogen treatment (Fig. 3).

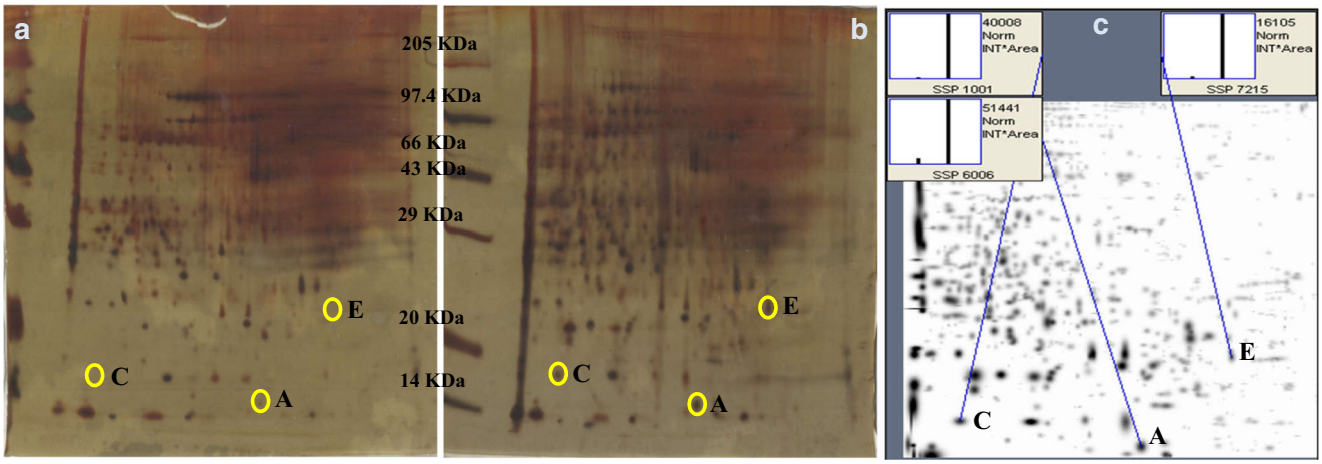

Fig. 1 Total tissue proteins were resolved on 2D gels of control (**A**) and treated (**B**) animals. Some of the differentially expressed protein spots (target proteins in this study) are marked as A, C, and E. (**C**) Master gel of control and 4th month in which the selected protein spots are given unique SSP numbers, namely, A: 6006; C: 1001; and E: 7215. The pop up graphs on master gel compared the protein expression based on intensity

Network analysis of genes coding for the experimentally identified proteins

Further study on these proteins demonstrated their association with a number of interacting partners indicating the contribution of these proteins in pathophysiology of HCC. We analyzed the functional association of the dysregulated genes coding for experimentally identified proteins and their interacting partners to deduce their possible role in HCC development. The resulting global gene network using functional GENEMANIA database (Fig. S1) (supplementary data) showed following observations:

1- Co-expression of MMP10 and MTG1; SYNE1 and KDR; MTG1 with MTOR, CUL7, CUL9, MMP10, and KLC1.
2- SYNE1 gene was found to interact with FOS, JUN, EGFR, VEGFA, MMP3, HGF, KLC1, ATF2, MLF2, FKLPB7, TELO2, MAPK8, MAPK9, and MAPKAP1.
3- The network analysis revealed direct interaction between MMP10 and MMP3, which further connect MPP10 to JUN, FOS, SYNE1, and EGFR; furthermore, JUN connects MMP10 to MAPK8, MAPK9, and TP53. The direct interaction among EGFR and MTOR has also been found. Moreover, the network also revealed the direct interaction of MTG1 with CUL7 and CUL9. These further connect MTG1 to FOS, JUN, EGFR, VEGFA through TP53 (Fig. 4) (Table 4).

Discussion

The report describes the elucidation of molecular events during HCC progression. Using proteomic and genomic approaches, we have investigated the possible role of the three proteins and their genes, namely, nesprin-1 isoform X6 (SYNE1), stromelysin-2 precursor (MMP10), and mitochondrial ribosome-associated GTPase 1-isoform X2 (MTG1). We report that these proteins interact with several signaling pathways involved in HCC development.

The level of nesprin-1 isoform X6 was found to be elevated. Nesprin-1 is an outer nuclear membrane protein that links the nucleus to actin cytoskeleton (Zhang et al 2009). It has been reported that nesprin-1 plays a critical role in cell proliferation and apoptosis of mesenchymal stem cells (MSCs) (Yang et al. 2013). SYNE1 is large gene (0.5 Mb) that encodes different isoforms of nesprin-1 by alternative splicing. This plays a critical role in cell structural integrity, cell signaling,

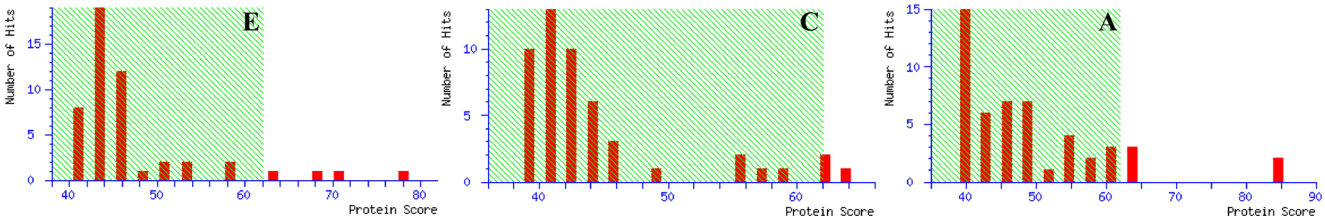

Fig. 2 Mascot Score Histogram of MALDI-TOF-MS-identified protein spots. The search against Mascot Score Histogram identified the proteins and the score for each protein is shown in this figure. Whereas spot E: Nesprin-1 isoform X6, spot C: Stromelysin-2 precursor and spot A: Mitochondrial ribosome-associated GTPase 1 isoform X2

Table 2 Name of characterized proteins by MALDI-TOF and their related genes

Spot name	Protein name	Gene name	Uniprot ID
E	Nesprin-1 isoform X6	SYNE1	Q8NF91
C	Stromelysin-2 precursor	MMP10	P09238
A	Mitochondrial ribosome-associated GTPase 1 isoform X2	MTG1	Q9BT17

and nuclear organization (Doherty et al. 2010). In contrary to our study, SYNE1 gene was found to be downregulated in ovarian cancer (Doherty et al. 2010) and oral cancer (Shah et al. 2018). On the other hand, our observations are in sync with several studies wherein SYNE1 gene has been reported to be upregulated in colorectal cancer (Melotte et al. 2015) and lung cancer (Tessema et al. 2008). Nuclear envelope encoding gene–associated mutations have been implicated as one of the important reasons of age-associated diseases and cancer (Kim et al. 2015). Mutations in SYNE1 have been reported to be associated with several cancers including head and neck squamous cell cancer (Eun et al. 2017), colorectal cancer (Jesinghaus et al. 2015), NAFLD-related HCC (Ki Kim S et al. 2016), glioblastoma (Masica and Karchin 2011), and gastric cancer (Cong et al. 2018).

Diane Zhang has reported the association of SYNE1, CLU7, and CUL9 to liver cancer (Zhang 2016). The represented data propose the interaction between SYNE1, CUL7, and CUL9 through p53 and VEGFR. It has been documented that function of CUL9 in tumor suppression is largely mediated through p53 whereas deletion of CUL9 had no significant effect on cell-cycle progression, but affected impaired DNA damage-induced apoptosis (Pei et al. 2011). On the other hand, SYNE1 has interaction with JUN and FOS. A study carried out on DEN-induced liver cancer-bearing mice showed that dysregulated expression of FOS is a key element occurring during HCC development that induces inflammation, hepatocyte proliferation, DNA damage response activation, and premalignant transformation (Latifa et al. 2017). Our study was performed on the liver with DEN-induced HCC whereas, DEN is a carcinogen which induces single-strand breaks in DNA in hepatocytes and also causes changes in several enzymes involved in DNA repair (Malik et al. 2013). All together, we conclude that high expression of SYNE1 may induce liver cancer formation through interactions with liver cancer-associated genes such as JUN, FOS, VEGFR, P53, CUL7, and CUL9 suggesting that SYNE1 could have a role in cancer development pathways.

Upregulation of stromelysin-2 (MMP10) expression has been reported in our study and its elevation is associated with HCC angiogenesis (García-Irigoyen et al. 2015). MMP10 is a cancer-related gene belonging to stromelysins (MMP-3, 7, 10, 11, 26, and 27) that displays hydrolyzing ability of a broad range of complex extracellular matrix (ECM) proteins like collagen type III, IV, V, elastin, proteoglycans, and glycoproteins (Zhang and Chen, 2017). Degradation and renewal of liver tissue are associated with the ECM-related pathways (Duarte et al. 2015). Many extracellular factors such as cytokines, growth factors, and cell contact to ECM regulate the expression of MMP genes (Westermarck and Kähäri, 1999). The invasion of MMP10 in head and neck squamous cell carcinoma is presumably associated with partial inhibition of p38 MAPK (Deraz et al. 2011). The p38α (MAPK14) has been speculated to directly affect tumor invasion and angiogenesis as it can induce expression of the matrix metalloproteinases such as MMP1, MMP3, and MMP13 which regulate matrix renewal and degradation by metastatic cancer cells whose subsequent activity is needed for HCC proliferation (Wagner and Nebreda, 2009). In the present study, the deduced network reveals the interaction of MMP3 with p53 through HGF, as well as cross-talk between MMP10 with JUN and FOS through MMP3, which connect MMP10 with MAPK8 and MAPK9 (Fig. 4). Stromelysin-1 (MMP-3) induces HGF-mediated invasion of HCC (Inserm 2002). There are several signal cascades that control the expression of MMP10 including MAPK and JAK/STAT pathways (Cui et al. 2012). MMP10 gene contains DNA-binding sites for AP-1 and STAT3 at the 5′ regulatory region (Cui et al. 2012). AP-1 is a dimer composed of FOS and JUN family members and its activity is regulated by interactions with some kinases and transcriptional co-activators (Karin et al. 1997). Co-expression of FOS and JUN is suspected to be associated with tumor progression in HCC (Yuen et al. 2001). Our observations correlate with another finding wherein JNK/JUN pathway was reported to target genes of metalloproteinases such as MMP10. The oncogenic functions of JNKs are mostly based on their ability to phosphorylate JUN and therefore, to activate AP-1; however, their suppression function is also related to their pro-apoptotic activity (Wagner and Nebreda, 2009). On the other hand, our network revealed interactions of MMP10 and STAT3 through MTG1 and MTOR, whereas STAT3 plays a pivotal role in HCC survival, growth, angiogenesis, and metastasis (Jung et al. 2017). Altogether, based on our data obtained from the network, we hypothesize that signal transduction among JNK/JUN and STAT3 may induce the enhanced expression of MMP10 through MMP3 leading to HCC progression by induction of angiogenesis.

Table 3 The peptide sequence analysis of SYNE1, MMP10, and MTG1 (*Mr*, average molecular mass of the peptide in kilodalton; *Expt*, experimentally determined molecular mass; *Calc*, theoretically calculated mass of peptide based on atomic mass; and *Ppm*, parts per million)

Observed	Mr (expt)	Mr (calc)	ppm	Start–End	Miss	Peptide
Nesprin X6 (SYNE1)						
640.3079	639.3006	639.2864	22.2	6594–6598	0	K.SQYDK.A
641.3145	640.3072	640.3293	− 34.40	5147–5151	0	K.LSEHR.A
699.3789	698.3717	698.3711	0.76	7235–7240	0	K.QLHSSK.A
868.5459	867.5386	867.4926	53.0	8673–8679	1	K.EVSRHIK.D
882.5865	881.5792	881.4970	93.2	8677–8683	1	R.HIKDLEK.L
913.5283	912.5211	912.5392	− 19.90	4671–4678	0	K.IQEAILAR.K
939.5763	938.5690	938.4934	80.6	1803–1810	0	R.DHQVALTR.H
955.5306	954.5233	954.5750	− 54.11	2905–2913	0	R.VELLAPSVK.Q
960.5394	959.5321	959.4825	51.7	8094–8100	1	R.WDDLQKR.V
969.5743	968.5671	968.5291	39.2	3811–3818	1	R.KEHVSLEK.G
973.5615	972.5543	972.5352	19.6	5954–5961	1	K.NVISEKQR.T
982.5629	981.5556	981.4767	80.4	2808–2815	1	K.KTQDESFK.E
987.5766	986.5693	986.5298	40.1	7007–7014	0	K.SWQLLQGR.V
989.5267	988.5194	988.5342	− 14.90	6734–6741	0	R.TSLYQHLK.S
994.5581	993.5508	993.5131	38.0	5962–5969	0	R.TLYEALER.Q
1033.5667	1032.5594	1032.4797	77.1	3017–3025	0	K.AEPMTEDLK.S
1051.6945	1050.6872	1050.5934	89.3	8658–8666	1	K.EKVHVIGNR.L
1057.5887	1056.5814	1056.6040	− 21.39	7560–7568	1	R.RGIIDSQIR.Q
1095.6826	1094.6753	1094.6084	61.1	5786–5794	1	R.HEELAQKIK.G
1107.5852	1106.5779	1106.5754	2.32	4500–4509	1	K.TCKTAQASLK.T
1111.6179	1110.6106	1110.5557	49.5	2146–2155	1	K.ELDSFTSKGK.H
1118.5812	1117.5739	1117.5550	16.9	7839–7847	0	K.IQLQQMGER.L + oxidation (M)
1157.6338	1156.6265	1156.5910	30.7	3761–3770	1	K.DMEKGHSLLK.S
1174.6494	1173.6422	1173.6063	30.5	7338–7347	0	R.LEALEQALCK.Q
1179.6334	1178.6262	1178.6118	12.2	4182–4190	1	K.DFIKQLQCK.Q
1201.6362	1200.6290	1200.6139	12.6	4295–4304	1	K.FAIDDLKDHK.Q
1225.6625	1224.6552	1224.6020	43.4	1894–1904	1	R.QTVEATKSMSK.K + oxidation (M)
1227.6779	1226.6706	1226.7347	− 52.23	3145–3156	1	K.AQAVQAKVLTAK.E
1229.6477	1228.6404	1228.6451	− 3.87	7225–7234	0	R.WNNLLEEIAK.Q
1234.6869	1233.6796	1233.5990	65.4	2068–2077	1	R.LEATWDDTKR.L
1254.6648	1253.6575	1253.6081	39.4	2422–2431	0	K.EFQEWFLGAK.A
1257.6986	1256.6913	1256.6360	44.0	7661–7671	1	K.SASTHLEEQKK.K
1303.7398	1302.7325	1302.6667	50.6	5377–5387	1	R.ESIEKIAEEQK.N
1306.7094	1305.7021	1305.6538	37.0	2375–2385	1	K.HHSVELESRGR.A
1308.6980	1307.6907	1307.5888	77.9	8074–8084	1	R.ENRTDSACSLR.Q
1320.6253	1319.6180	1319.651	− 25.00	6842–6852	0	R.DHLNAFLEFSK.E
1341.7156	1340.7083	1340.7313	− 17.15	3495–3504	1	K.LVRLHQEYQR.D
1383.7142	1382.7069	1382.7082	− 0.89	7607–7617	1	R.TLFDEVQFKEK.V
1410.7453	1409.7380	1409.8354	− 69.12	685–696	1	R.DLKQQLLLLNGR.W
1419.7425	1418.7352	1418.7439	− 6.09	3170–3181	1	K.ESALENLKIQMK.D + oxidation (M)
1432.7657	1431.7584	1431.7722	− 9.60	6488–6499	0	R.LQQVLSFQNDLK.V
1434.7895	1433.7823	1433.7303	36.3	329–339	1	K.EAKVWIEQFER.D
1446.7739	1445.7667	1445.7990	− 22.39	3812–3824	1	K.EHVSLEKGVHLAK.E
1468.7481	1467.7409	1467.7542	− 9.10	6229–6240	1	R.THQRQSSLQQQK.E
1475.7652	1474.7579	1474.7449	8.78	4305–4316	1	K.QKLMEQLSLDDR.E
1493.7614	1492.7541	1492.7782	− 16.13	763–775	1	R.VPVMDAQYKMIAK.K
1527.7752	1526.7679	1526.8569	− 58.27	7542–7554	0	K.LTLLSNQWQGVIR.R
1544.8020	1543.7947	1543.8358	− 26.63	7418–7430	1	R.LNELGYRLPLNDK.E
1555.8110	1554.8038	1554.8075	− 2.43	5678–5690	0	R.QHLLSEMESLKPK.V + oxidation (M)
1584.7468	1583.7396	1583.7514	− 7.51	7765–7776	0	R.QWEELCHQVSLR.R
1657.8224	1656.8151	1656.8570	− 25.31	6599–6613	0	K.ALQDLVDLLDTGQEK.M
1683.8785	1682.8712	1682.9580	− 51.58	7542–7555	1	K.LTLLSNQWQGVIRR.A
1707.8008	1706.7936	1706.9580	− 96.33	7235–7248	1	K.QLHSSKALLQLWQR.Y
1808.9358	1807.9286	1807.9138	8.16	1788–1802	0	K.QFLSELQMTSEINLR.D
1838.9189	1837.9116	1837.8305	44.1	3612–3625	1	K.FQEADEWLQRMEEK.I
1853.9487	1852.9414	1852.9366	2.59	7867–7881	1	K.VNDRWQHLLDLMAAR.V + oxidation (M)
1868.9337	1867.9264	1867.8478	42.1	5984–5999	1	K.MEAMEMKLSESLQPGR.S + 2 oxidation (M)
1881.9256	1880.9183	1880.8653	28.2	6441–6456	1	K.NKNLFSQAFPEDSDNR.D
1924.9632	1923.9559	1923.8884	35.1	2174–2189	1	K.TDMESTLDKWLDVSER.I
1940.9356	1939.9283	1939.8833	23.2	2174–2189	1	K.TDMESTLDKWLDVSER.I + oxidation (M)
1999.0160	1998.0087	1997.9186	45.1	478–495	0	R.SVNGIPMPPDQLEDMAER.F

Table 3 (continued)

Observed	Mr (expt)	Mr (calc)	ppm	Start–End	Miss	Peptide
2003.9376	2002.9303	2002.9232	3.57	3926–3941	1	K.VRDHEDYNTELQEVEK.W
2022.9711	2021.9638	2021.9324	15.5	8349–8366	1	R.NTSGDPTSLESQMRQLDK.A + oxidation (M).
2082.9759	2081.9686	2082.0018	− 15.93	3387–3404	1	K.SQLEGALSKWTSYQDDVR.Q
2189.0599	2188.0526	2188.1272	− 34.06	6919–6937	0	R.HAISEVMSWISLMESVILK.D + oxidation (M)
2211.0744	2210.0671	2210.0069	27.3	1453–1470	0	K.WDHFGSNFETLSNWITEK.E
2225.0995	2224.0923	2224.1409	− 21.87	8521–8540	1	R.KAIILSINLCSSEFTQADSK.E
2239.1022	2238.0950	2238.1855	− 40.47	3562–3581	1	R.EDVILSGLPQAEDRVLESLR.Q
2383.9327	2382.9255	2383.1148	− 79.44	5422–5441	1	K.VQEIEQGKAMSQEFSCQIQK.V + oxidation (M)
2680.2131	2679.2058	2679.3061	− 37.43	5524–5546	1	R.LSKLNQASSHLEEYSEMLESIQK.W + oxidation (M)
2705.1389	2704.1316	2704.3490	− 80.38	6315–6336	1	K.QKLLQNILEQEQEQMLYSSPNR.L + oxidation (M)
2763.3357	2762.3284	2762.2970	11.4	4238–4260	1	R.EQDLQRTSSYHDHMSIVEAFLEK.F
2908.4005	2907.3932	2907.3960	− 0.94	5527–5550	1	K.LNQASSHLEEYSEMLESIQKWIEK.A + oxidation (M)
Stomylysin − 2 precoursor (MMP10)						
987.5826	986.5754	986.5760	− 0.67	55–63	2	R.KDSSPVVKK.I
1107.5639	1106.5566	1106.5543	2.12	415–423	1	R.QLMDKGFPR+.L oxidation (M)
1157.6202	1156.6129	1156.5587	46.9	233–241	0	K.ESLMYPVYR.F
1259.6926	1258.6853	1258.6683	13.6	109–117	2	K.WRKNHISYR.I
1277.7120	1276.7047	1276.7027	1.61	387–397	2	K.IDAAVFEKEKK.K
1282.6771	1281.6698	1281.6023	52.6	410–419	1	R.FDETRQLMDK.G
1365.6704	1364.6631	1364.7929	− 95.07	374–385	1	K.RIHTLGFPPTVK.K
1493.7380	1492.7307	1492.8878	− 105.23	374–386	2	K.RIHTLGFPPTVKK.I
1610.8276	1611.8349	1610.7433	52.4	289–302	0	K.CDPALSFDAVTMLR.G + oxidation (M)
1753.9018	1752.8945	1752.8790	8.86	64–78	1	K.IEEMQKFLGLEMTGK.L
1803.9067	1802.8994	1802.8410	32.4	407–419	2	K.YWRFDETRQLMDK.G + oxidation (M)
1993.9437	1992.9364	1992.9806	− 22.17	356–373	1	K.GSQFWAVRGNEVQAGYPK.R
2150.0279	2149.0206	2149.0817	− 28.42	356–374	2	K.GSQFWAVRGNEVQAGYPKR.I
2211.0469	2210.0396	2210.2463	− 93.54	375–394	2	R.IHTLGFPPTVKKIDAAVFEK.E
2566.2118	2565.2046	2565.2389	− 13.40	70–91	1	K.FLGLEMTGKLDSNTVEMMHKPR.C + 2 oxidation (M)
2762.2762	2761.2690	2761.4286	− 57.82	128–151	2	R.ESVDSAIERALKVWEEVTPLTFSR.I
Mitochondrial ribosome-associated GTPase 1 isoform X2						
709.3396	708.3323	708.3476	− 21.63	41–46	0	K.MQSSLK.L + oxidation (M)
842.5224	841.5152	841.5385	− 27.75	270–277	1	K.NVAIKLGK.T
973.5588	972.5516	972.4640	90.0	29–36	0	R.WFPGHMAK.G
989.5416	988.5344	988.4589	76.3	29–36	0	R.WFPGHMAK.G + oxidation (M)
1182.6499	1044.5864	1044.6040	− 16.82	156–164	1	K.SSLINSLRR.Q
1108.5867	1107.5794	1107.5747	4.32	106–114	0	R.NVIFTNCIK.D
1183.6572	1045.5937	1182.6469	2.56	172–183	1	K.AARVGGEPGITR.A
1197.6548	1196.6475	1196.6765	− 24.16	115–124	1	K.DENIKQIIPK.V
1307.7252	1306.7179	1306.6075	84.5	84–94	0	K.MDLADLTEQQK.I + oxidation (M)
1425.7470	1424.7397	1424.7082	22.1	47–58	0	K.LVDCVIEVHDAR.I
1434.8146	1433.8073	1433.7813	18.1	103–114	1	K.GLRNVIFTNCIK.D
1598.8577	1597.8504	1597.8154	21.9	3–16	0	R.LWPQAWSAVGAAWR.E
1707.8277	1706.8204	1706.8661	− 26.77	106–119	1	R.NVIFTNCIKDENIK.Q
1991.9984	1990.9912	1990.9492	21.1	138–155	0	R.AENPEYCIMVVGVPNVGK.S + oxidation (M)
2083.0363	2082.0290	2082.0681	− 18.75	47–64	1	K.LVDCVIEVHDARIPFSGR.N
2284.1597	2283.1524	2283.1416	4.74	84–102	1	K.MDLADLTEQQKIVQHLEEK.G + oxidation (M)
2299.1667	2298.1594	2298.2696	− 47.93	281–302	1	K.VKVLTGTGNVNVIQPDYAIAAR.D
2399.0621	2398.0548	2398.1099	− 22.99	17–36	1	R.ECFPLQGHDVARWFPGHMAK.G + oxidation (M)

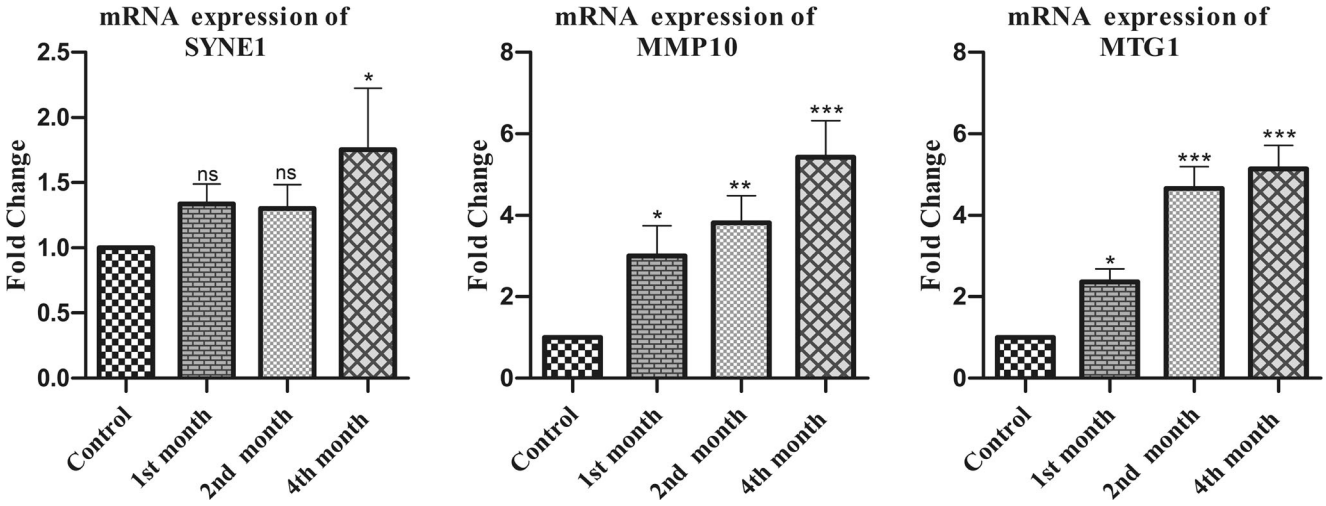

Fig. 3 Expression analysis of SYNE1, MMP10, and GTPase1 in control and carcinogen-treated groups by real-time PCR

We also report an increase in the mitochondrial ribosome-associated GTPase 1 expression in our study. The generated network revealed direct interactions among MTG1 with MMP10 and with MTOR, CUL7, and CUL9. MTG1 is potentially associated with several cancers; however, further studies are needed to find out the exact role of this protein in cancer induction or progression (Liu and Pan 2016). MTG1 plays a role in regulation of mitochondrial ribosome assembly and translational activity (Kotani et al. 2013).

According to GENE CARD database (www.genecards.org), Gene Ontology shows the annotations related to MTG1, which includes GTP binding and GTPase activity. Certain small GTP-binding proteins control the enzymatic activity of mitogen-activated protein kinases (MAPKs) such as ERKs, JNKs, and p38 kinase subfamilies (Teramoto et al. 1996) in signaling pathways associated with cancer progression (Latifa et al. 2017). The present study shows the interactions of MTG1 with MAPK8 and MAPK9 through MTOR. We may conclude that MTG1 may have a role in HCC formation through its relation with MAPKs and JNKs.

Altogether, we conclude that elevation in expression of SYNE1, MMP10, and MTG1 may play critical role in HCC development through their interrelationship with CUL 7 and 9, TP53, VEGFR, JNK/JUN, STAT3, FOS, MAPKs, MTOR, and HGF.

Conclusion

Three proteins, namely SYNE1, MMP10, and MTG1 have been found to be overexpressed in HCC and the interactions among these are shown to be through JUN, STAT3, FOS, TP53, VEGFR, CUL9, CUL7, HGF, and MAPKs Table 4. These proteins play pivotal regulatory roles in signaling pathways associaed with HCC progression and thus could be

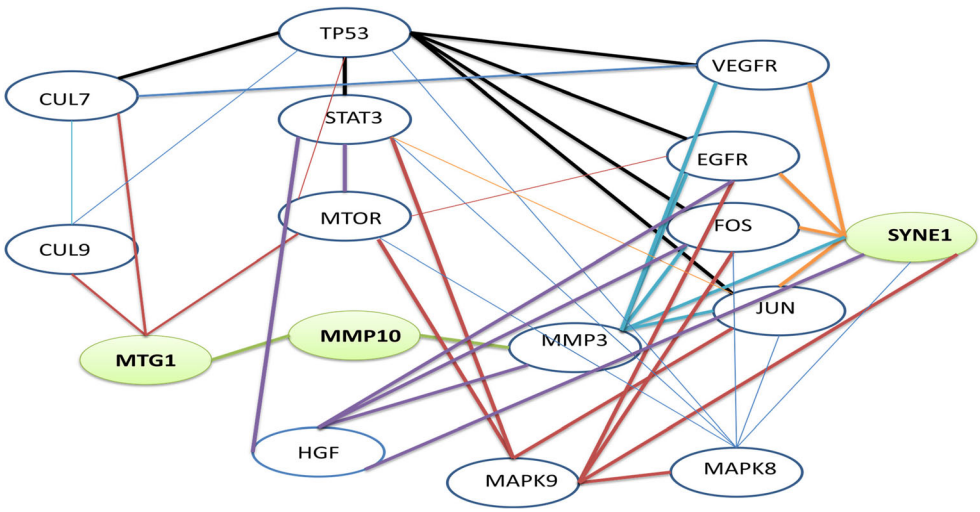

Fig. 4 Network diagram showing interactions among the gene coding for identified proteins and their neighbors involve in cancer pathways

Table 4 The significant reported HCC-associated genes showing interactions with SYNE1, MMP10, and MTG1

Protein name	Gene name	Uniprot ID	References
Serine/threonine-protein kinase mTOR	MTOR	P42345	(Matter et al. 2014)
Signal transducer and activator of transcription 3	STAT3	P40763	(Xie et al. 2018; Li et al. 2017)
Mitogen-activated protein kinase 8	MAPK8	P45983	(Han et al. 2016)
Mitogen-activated protein kinase 9	MAPK9	P45984	(Chan et al. 2017; Zhang et al. 2019)
Cullin-7	CUL7	Q14999	(Paradis et al. 2013)
Cullin-9	CUL9	Q8IWT3	(Zhang 2016)
Cellular tumor antigen p53	TP53	P04637	(Zhang et al. 2019; Meng et al. 2014)
Vascular endothelial growth factor A	VEGFA	P15692	(Cheng et al. 2018)
Epidermal growth factor receptor	EGFR	P00533	(Huang et al. 2014)
Proto-oncogene c-Fos	FOS	P01100	(Bakiri et al. 2017)
Transcription factor AP-1	JUN	P05412	(El-tawdi et al. 2016)
Hepatocyte growth factor receptor	HGF	P08581	(Goyal et al. 2013)
Stromelysin-1	MMP3	P08254	(Monvoisin et al. 2002b; Cui et al. 2011)

targeted as potential biomarkers for early detection of HCC. However, further research is needed to validate the data obtained from this study using human samples.

Acknowledgments The authors are grateful to Jamia Hamdard for providing necessary facilities for this study.

The financial assistance by Ministry of Education, Libya, in form of a fellowship to L.S. is gratefully acknowledged.

Author contribution statement All authors have contributed equally and approved the final manuscript.

Laila H Faraj Shaglouf conducted all the experiments, collected the data, analyzed the data, and wrote the manuscript. Dr. Maryam Ranjpour has induced the model and helped in reviewing the manuscript. Dr. Saima Wajid helped in conducting the experiments, analyzing the data, and reviewing the manuscript. Prof. S.K. Jain has designed and conceptualized the study, provided research facilities, analyzed the data, reviewed, and finalized the manuscript.

Financial support The work was financially supported by a MRP grant from UGC to S K Jain (Grant no. 40-155/2011(SR)), New Delhi, India.

Compliance with ethical standards

Conflict of interest The authors declare that they have no conflict of interests.

References

Aravalli RN, Cressman EN, Steer CJ (2013) Cellular and molecular mechanisms of hepatocellular carcinoma: an update. Arch Toxicol 87:227–247

Avila MA, Berasain C, Sangro B, Prieto J (2006) New therapies for hepatocellular carcinoma. Oncogene 25:3866–3884

Bakiri L, Hamacher R, Graña O, Guío-Carrión A, Campos-Olivas R, Martinez L, Dienes HP, Thomsen MK, Hasenfuss SC, Wagner EF (2017) Liver carcinogenesis by FOS-dependent inflammation and cholesterol dysregulation. J Exp Med 214:1387–1409

Bradford MM (1976) A rapid and sensitive method for the quantitation of microgram quantities of protein utilizing the principle of protein-dye binding. Anal Biochem 72:248–254

Bray F, Ferlay J, Soerjomataram I et al (2018) Global cancer statistics 2018: GLOBOCAN estimates of incidence and mortality worldwide for 36 cancers in 185 countries Freddie. CA Cancer J Clin 68:394–424

Chaudhary N, Bhatnagar S, Malik S, Katare DP, Jain SK (2013) Proteomic analysis of differentially expressed proteins in lung cancer in Wistar rats using NNK as an inducer. Chem Biol Interact 204: 125–134

Cheng S, Zhang X, Xu Y, Dai X, Li J, Zhang T, Chen X (2018) Krüppel-like factor 8 regulates VEGFA 325 expression and angiogenesis in hepatocellular carcinoma Scientific reports 8326 doi:10.1038/s41598-018-35786-6

Chiba T, Suzuki E, Saito T, Ogasawara S, Ooka Y, Tawada A, Iwama A, Yokosuka O (2015) Biological features and biomarkers in hepatocellular carcinoma. World J Hepatol 7:2020–2028

Cong T, Liu GX, Cui JX, Zhang KC, Chen ZD, Chen L, Wei B, Huang XH (2018) Exome sequencing of gastric cancers screened the differences of clinicopathological phenotypes between the mutant and the wide-type of frequently mutated genes. Zhonghua Yi Xue Za Zhi 98:2242–2245

Cui C et al (2011) CRP promotes MMP-10 expression via c-Raf/MEK/ERK and JAK1/ERK pathways in cardiomyocytes. Cell Signal 24: 810–818. https://doi.org/10.1016/j.cellsig.2011.11.019

Dalton ND, Guo LT, Shelton GD et al (2009) Nesprin 1 is critical for nuclear positioning and anchorage. Hum Mol Genet 19:329–341

De Minicis S, Marzioni M, Benedetti A (2013) New insights in hepatocellular carcinoma : from bench to bedside. Ann Transl Med 1:1–11

Deraz EM, Kudo Y, Yoshida M, Obayashi M, Tsunematsu T, Tani H, Siriwardena SBSM, Kiekhaee MR, Qi G, Iizuka S, Ogawa I, Campisi G, Muzio LL, Abiko Y, Kikuchi A, Takata T (2011) MMP-10/stromelysin-2 promotes invasion of head and neck cancer. PLoS One 6:e25438

Doherty AJ, Rossing MA, Haugen KLC et al (2010) ESR1/SYNE1 polymorphism and invasive epithelial ovarian cancer risk: an ovarian cancer association consortium study. Cancer Epidemiol Biomark Prev 19:245–251

Duarte S, Baber J, Fujii T, Coito AJ (2015) Matrix metalloproteinases in liver injury, repair and fibrosis. Matrix Biol 44:147–156

El-Tawdi AH, Matboli M, El-Nakeep S, Azazy AE, Abdel-Rahman O (2016) Association of long noncoding RNA and c-JUN expression in hepatocellular carcinoma. Expert Rev Gastroenterol & Hepatol 10:869–877. https://doi.org/10.1080/17474124.2016.1193003

Eun Y-G, Lee D, Lee YC, Sohn BH, Kim EH, Yim SY, Kwon KH, Lee JS (2017) Clinical significance of YAP1 activation in head and neck squamous cell carcinoma. Oncotarget 8:111130–111143

García-Irigoyen O, Latasa MU, Carotti S et al (2015) Matrix metalloproteinase 10 contributes to hepatocarcinogenesis in a novel crosstalk with the stromal derived factor 1/C-X-C chemokine receptor 4 axis. Hepatology 62:166–178

Goyal L, Muzumdar MD, Zhu AX (2013) Targeting the HGF/c-MET pathway in hepatocellular carcinoma. Clin Cancer Res 19:2310–2318. https://doi.org/10.1158/1078-0432.ccr-12-2791

Han MS, Barrett T, Brehm MA, Davis RJ (2016) Inflammation mediated by JNK in myeloid cells promotes the development of hepatitis and hepatocellular carcinoma. Cell Rep 15:19–26. https://doi.org/10.1016/j.celrep.2016.03.008

Hemming AW, Berumen J, Mekeel K (2016) Hepatitis B and hepatocellular carcinoma. Clin Liver Dis 20:703–720

Huang P, Xu X, Wang L, Zhu B, Wang X, Xia J (2014) The role of EGF-EGFR signalling pathway in hepatocellular carcinoma inflammatory microenvironment. J Cell Mol Med 18:218–230. https://doi.org/10.1111/jcmm.12153

Inserm E (2002) Involvement of matrix metalloproteinase type-3 in hepatocyte growth factor-induced invasion of human hepatocellular. Int J Cancer 162:157–162

Jesinghaus M, Wolf T, Pfarr N, Muckenhuber A, Ahadova A, Warth A, Goeppert B, Sers C, Kloor M, Endris V, Stenzinger A, Weichert W (2015) Distinctive spatiotemporal stability of somatic mutations in metastasized microsatellite-stable colorectal cancer. Am J Surg Pathol 39:1140–1147

Jung KH, Yoo W, Stevenson HL, Deshpande D, Shen H, Gagea M, Yoo SY, Wang J, Eckols TK, Bharadwaj U, Tweardy DJ, Beretta L (2017) Multifunctional effects of a small-molecule STAT3 inhibitor on NASH and hepatocellular carcinoma in mice. Clin Cancer Res 23:5537–5546

Karin M, Liu Z, Zandi E (1997) AP-1 function and regulation. Curr Opin Cell Biol 9:240–246

Ki Kim S et al (2016) TERT promoter mutations and chromosome 8p loss are characteristic of nonalcoholic fatty liver disease-related hepatocellular carcinoma. Int J Cancer 139:2512–2518. https://doi.org/10.1002/ijc.30379

Kim GA, Lee HC, Kim MJ, Ha Y, Park EJ, An J, Lee D, Shim JH, Kim KM, Lim YS (2015) Incidence of hepatocellular carcinoma after HBsAg seroclearance in chronic hepatitis B patients: a need for surveillance. J Hepatol 62:1092–1099

Kim SK, Ueda Y, Hatano E et al (2016) Short report characteristic of nonalcoholic fatty liver disease-related hepatocellular carcinoma. Int J Cancer Short 2518:2512–2518

Kotani T, Akabane S, Takeyasu K, Ueda T, Takeuchi N (2013) Human G-proteins, ObgH1 and Mtg1, associate with the large mitochondrial ribosome subunit and are involved in translation and assembly of respiratory complexes. Nucleic Acids Res 41:3713–3722

Li M et al (2017) STAT3 regulates glycolysis via targeting hexokinase 2 in hepatocellular carcinoma cells. Oncotarget 8:24777–24784. https://doi.org/10.18632/oncotarget.15801

Liu X, Pan L (2016) Predicating candidate cancer-associated genes in the human signaling network using centrality. Curr Bioinforma 11:87–92

Malik S, Bhatnagar S, Chaudhary N, Katare DP, Jain SK (2013) DEN+2-AAF-induced multistep hepatotumorigenesis in Wistar rats: supportive evidence and insights. Protoplasma 250:175–183

Masica DL, Karchin R (2011) Correlation of somatic mutation and expression identifies genes important in human glioblastoma progression and survival. Cancer Res 71:4550–4561

Matter MS, Decaens T, Andersen JB, Thorgeirsson SS (2014) Targeting the mTOR pathway in hepatocellular carcinoma: current state and future trends Journal of hepatology 60:855-865 https://doi.org/10.1016/j.jhep.2013.11.031

Melotte V, Yi JM, Lentjes MHFM, Smits KM, van Neste L, Niessen HEC, Wouters KAD, Louwagie J, Schuebel KE, Herman JG, Baylin SB, van Criekinge W, Meijer GA, Ahuja N, van Engeland M (2015) Spectrin repeat containing nuclear envelope 1 and forkhead box protein E1 are promising markers for the detection of colorectal cancer in blood. Cancer Prev Res 8:157–164

Meng X, Franklin DA, Dong J, Zhang Y (2014) MDM2-p53 pathway in hepatocellular carcinoma. Cancer Res 74:7161–7167. https://doi.org/10.1158/0008-5472.can-14-1446

Paradis V et al (2013) Cullin7: a new gene involved in liver carcinogenesis related to metabolic syndrome. Gut 62:911–919. https://doi.org/10.1136/gutjnl-2012-302091

Pei X, Bai F, Li Z et al (2011) Cytoplasmic CUL9/PARC ubiquitin ligase is a tumor suppressor and promotes p53-dependent apoptosis. Cancer Res 71:2969–2978

Ranjpour M, Katare DP, Wajid S, Jain SK (2018) HCC specific protein network involving interactions of EGFR with A-Raf and transthyretin : experimental analysis and computational biology correlates. Anti Cancer Agents Med Chem 18:1–14

Ranjpour M, Wajid S, Jain SK (2019) Elevated expression of A-Raf and FA2H in hepatocellular carcinoma is associated with lipid metabolism dysregulation and Cancer progression. Anti Cancer Agents Med Chem 19:236–247. https://doi.org/10.2174/1871520618666181015142810

Sever R, Brugge JS (2015) Signal transduction in cancer. Cold Spring Harb Perspect Med 5:a006098

Shah K, Patel S, Modi B, Shah F, Rawal R (2018) Uncovering the potential of CD44v/SYNE1/miR34a axis in salivary fluids of oral cancer patients. J Oral Pathol Med 47:345–352

Stidley CA, Van Neste L, Tessema M et al (2008) Promoter methylation of genes in and around the candidate lung cancer susceptibility locus 6q23-25. Cancer Res 68:1707–1714

Tessema M et al (2008) Promoter methylation of genes in and around the candidate lung cancer susceptibility locus 6q23-25. Cancer Res 68:1707–1714. https://doi.org/10.1158/0008-5472.can-07-6325

Teramoto H, Crespo P, Coso OA, Igishi T, Xu N, Gutkind JS (1996) The small GTP-binding protein rho activates c-Jun N-terminal kinases/stress-activated protein kinases in human kidney 293T. J Biol Chem 271:25731–25735

Wagner EF, Nebreda ÁR (2009) Signal integration by JNK and p38 MAPK pathways in cancer development. Nat Rev Cancer 9:537–549

Warde-Farley D, Donaldson SL, Comes O et al (2010) The GeneMANIA prediction server: biological network integration for gene prioritization and predicting gene function. Nucleic Acids Res 38:214–220

Westermarck J, Kähäri VM (1999) Regulation of matrix metalloproteinase expression in tumor invasion. J Fed Am Soc Exp Biol 13:781–792

Yang W, Zheng H, Wang Y et al (2013) Nesprin-1 plays an important role in the proliferation and apoptosis of mesenchymal stem cells. Int J Mol Med 32:805–812

Xie Y, Li J, Zhang C (2018) STAT3 promotes the proliferation and migration of hepatocellular carcinoma cells by regulating AKT2. Oncol Lett 15:3333–3338. https://doi.org/10.3892/ol.2017.7681

Younes R, Bugianesi E (2018) Should we undertake surveillance for HCC in patients with NAFLD? J Hepatol 68:326–334

Yuen MF, Wu PC, Lai VCH, Lau JYN, Lai CL (2001) Expression of c-myc, c-fos, and c-jun in hepatocellular carcinoma. Cancer 91:106–112

Zhang D (2016) Copy number variations and their impact on gene expression in liver cancer. Columbia Undergrad Sci J 13:10506

Zhang J et al (2009) Nesprin 1 is critical for nuclear positioning and anchorage. Hum Mol Genet 19:329–341. https://doi.org/10.1093/hmg/ddp499

Zhang L, Li S, Wang R, Chen C, Ma W, Cai H (2019) Cytokine augments the sorafenib-induced apoptosis in Huh7 liver cancer cell by inducing mitochondrial fragmentation and activating MAPK-JNK signalling pathway. Biomed Pharmacother 110:213–223. https://doi.org/10.1016/j.biopha.2018.11.037

Zhang Y, Chen Q (2017) Relationship between matrix metalloproteinases and the occurrence and development of ovarian cancer. Brazilian J Med Biol Res 50:6–13